International Applied Mechanics, Vol. 47, No. 4, October, 2011 (Russian Original Vol. 47, No. 4, July, 2011)

DETERMINING THE NATURAL FREQUENCIES OF AN ELASTIC PARALLELEPIPED BY THE ADVANCED KANTOROVICH–VLASOV METHOD

E. I. Bespalova

An approach to calculate the natural frequencies of an elastic parallelepiped with different boundary conditions is proposed. The approach rationally combines the inverse-iteration method of successive approximations and the advanced Kantorovich–Vlasov method. The efficiency of the approach (the accuracy of the results and the number of approximating functions) is demonstrated against the Ritz method with different basis systems, including B-splines. The dependence of the lower frequencies of a three-dimensional cantilever beam on its cross-sectional dimensions is examined

Keywords: isotropic elastic parallelepiped, different boundary conditions, natural frequency, advanced Kantorovich–Vlasov method

Introduction. The present study was inspired by the paper [15] where the Ritz method with B-splines as basis functions was tested by calculating the natural frequencies of a rectangular parallelepiped. The vibrations of elastic bodies of such shape are addressed in a great number of Ukrainian and foreign publications reviewed in [15] and [3] with reference to isotropic and anisotropic materials, respectively.

The spectrum of natural frequencies of a parallelepiped with four sides hinged was analyzed in detail in [1, 11, 16] using trigonometric Fourier series expansion. Other types of boundary conditions can be examined by using analytical and numerical methods. Many relevant publications employ the Ritz method with emphasis on the selection of systems of basis functions. As such, power functions, simple and orthogonal polynomials, Chebyshev polynomials, etc. are used [10, 12–14, 17].

The methods that use finitely supported functions as basis systems occupy a special place in the class of Ritz methods. This approach gave rise to numerous modifications of the finite-element method having many applications. Among such methods are B-splines which have become popular recently. The results obtained with the Ritz method for various basis systems, including B-splines, were compared in [15] by solving three-dimensional eigenvalue problems for an isotropic parallelepiped.

B-splines in combination with the Kantorovich–Vlasov method were employed in [6–9] to reduce two-dimensional boundary-value and eigenvalue problems to ordinary differential equations. Unlike the Ritz method where approximating functions with respect to all variables of the domain are chosen beforehand, this approach makes it possible to find the functional coefficients of B-splines from the solution of the original problem. The efficiency of this method was tested against a wide class of two-dimensional problems for shells and plates.

To determine the natural frequencies of an isotropic parallelepiped, we will use the advanced Kantorovich–Vlasov method (AKM) for three-dimensional problems of elasticity. Such an approach to two-dimensional stationary problems for shallow shells was outlined in [4]. The AKM was used in [5] to solve the problem of twisting of a rectangular anisotropic prism.

1. Problem Formulation and Problem-Solving Method. Consider an elastic body in the form of a rectangular parallelepiped that occupies the domain $S \cup \partial S = \{x, y, z: x \in [0, a],\ y \in [0, b],\ z \in [0, c]\}$ in a Cartesian coordinate system x, y, z. The faces $z = 0,\ z = c$ are free of stresses, while the sides $x = 0,\ x = a$, and $y = 0,\ y = b$ are subject to arbitrary physically consistent combinations of stresses and displacements.

S. P. Timoshenko Institute of Mechanics, National Academy of Sciences of Ukraine, 3 Nesterov St., Kyiv, Ukraine 03057, e-mail: metod@inmech.kiev.ua. Translated from Prikladnaya Mekhanika, Vol. 47, No. 4, pp. 76–88, July 2011. Original article submitted March 15, 2010.

To determine the natural frequencies and modes of the parallelepiped, we have to solve the following generalized three-dimensional eigenvalue problem:

$$L\overline{U} - \lambda B\overline{U} = 0 \quad (x, y, z) \in S,$$

$$R\overline{U} = 0 \quad (x, y, z) \in \partial S, \tag{1.1}$$

where $L = D^{\mathrm{T}} CD$ is a matrix differential operator derived from the constitutive equations of anisotropic elasticity; $\lambda = \omega^2$ is an unknown numerical coefficient that has the sense of the squared natural frequency; $\overline{U} = \{u_p(x, y, z)\}_{p=1,2,3}$ is the displacement vector characterizing a vibration mode; $B = \{b_{ii} = \rho(x, y, z)\}$ $(i = 1, 2, 3)$ is the diagonal density matrix; R is the differential or algebraic matrix operator of boundary conditions;

$$D^{\mathrm{T}} = \begin{pmatrix} \partial/\partial x & 0 & 0 & 0 & \partial/\partial z & \partial/\partial y \\ 0 & \partial/\partial y & 0 & \partial/\partial z & 0 & \partial/\partial x \\ 0 & 0 & \partial/\partial z & \partial/\partial y & \partial/\partial x & 0 \end{pmatrix},$$

$C = \{c_{ij}\}$ $(i, j = \overline{1, 6})$ is the stiffness matrix of the generalized Hooke's law $\overline{\sigma} = C\overline{\varepsilon}$, $\overline{\sigma} = \{\sigma_{11}, \sigma_{22}, \sigma_{33}, \sigma_{23}, \sigma_{13}, \sigma_{12}\}$ and $\overline{\varepsilon} = \{\varepsilon_{11}, \varepsilon_{22}, \varepsilon_{33}, \varepsilon_{23}, \varepsilon_{13}, \varepsilon_{12}\}$ are the stress and strain vectors formally composed of the components of the associated tensors with allowance for their symmetry; for an isotropic material with shear modulus G and Poisson's ratio μ, the nonzero coefficients of the matrix $C = \{c_{ij}\}$ are $c_{ii} = 2G\dfrac{1-\mu}{1-2\mu}$, $c_{ij} = \dfrac{\mu}{1-\mu} c_{ii}$ $(i, j = 1, 2, 3)$, $c_{ii} = G$ $(i = 4, 5, 6)$; the indices "1," "2," "3" correspond to the coordinates x, y, z, respectively; all the vectors are column vectors.

To solve problem (1.1), we will follow an approach that rationally combines the inverse-iteration method of successive approximations [2] and the advanced Kantorovich–Vlasov method [4, 5]. The approach involves the following steps:

(i) reduction of the original homogeneous problem (1.1) with unknown numerical parameter λ to a sequence of inhomogeneous boundary-value problems of the same dimension using the method of successive approximations;

(ii) solution of each three-dimensional boundary-value problem of the sequence with the advanced Kantorovich–Vlasov method;

(iii) generation of a new iteration process for solving problem (1.1) and determination of the eigenvalues and associated vector functions.

At the first stage, according to the inverse-iteration method, we introduce a sequence of vector functions $\overline{V}^n$ as follows: $\overline{U} = \overline{V}^n$, $\lambda\overline{U} = \overline{V}^{n-1}$. As a result, with the spectrum of eigenvalues shifted by τ $(\lambda \to \lambda + \tau)$, the original problem (1.1) is reduced to a sequence of three-dimensional inhomogeneous boundary-value problems:

$$(L - \tau B)\overline{V}^n - B\overline{V}^{n-1} = 0 \quad (x, y, z) \in S,$$

$$R\overline{V}^n = 0 \quad (x, y, z) \in \partial S \quad (n = 1, 2, \ldots). \tag{1.2}$$

Using the known Rayleigh quotient [2] and the solutions $\overline{V}^n$ $(n = 1, 2, \ldots)$ of problems (1.2), we construct a numerical sequence:

$$\lambda_n = \frac{\int\limits_S (\overline{V}^n)^{\mathrm{T}} (L - \tau B)\overline{V}^n \, dxdydz}{\int\limits_S (\overline{V}^n)^{\mathrm{T}} B\overline{V}^n \, dxdydz} \qquad (n = 1, 2, 3), \tag{1.3}$$

that converges to the sought eigenvalue λ $(\lambda_n \to \lambda, n \to \infty)$. Any vector function of general form can be used as the initial approximation $\overline{V}^0$.

At the second stage, the nth problem of sequence (1.2) (n is fixed) is solved with the advanced Kantorovich–Vlasov method. To this end, the sought vector $\overline{V}^n = \{v_1^n, v_2^n, v_3^n\}$ is approximated by a vector $\overline{F}_M^n = \{f_{1M}^n, f_{2M}^n, f_{3M}^n\}$ as follows:

$$v_1^n(x,y,z) \simeq f_{1M}^n(x,y,z) = \sum_{i=1}^{M} X_{1i}^n(x) Y_{1i}^n(y) Z_{1i}^n(z),$$

$$v_2^n(x,y,z) \simeq f_{2M}^n(x,y,z) = \sum_{i=1}^{M} X_{2i}^n(x) Y_{2i}^n(y) Z_{2i}^n(z),$$

$$v_3^n(x,y,z) \simeq f_{3M}^n(x,y,z) = \sum_{i=1}^{M} X_{3i}^n(x) Y_{3i}^n(y) Z_{3i}^n(z), \tag{1.4}$$

where all the functions $X_{1i}^n(x)$, $X_{2i}^n(x)$, $X_{3i}^n(x)$, $Y_{1i}^n(y)$, $Y_{2i}^n(y)$, Y_{3i}^n, $Z_{1i}^n(z)$, $Z_{2i}^n(z)$, $Z_{3i}^n(z)$ $(i = \overline{1,M})$ dependent on different variables of the domain S are assumed to be unknown; M is the number of terms in the approximating expression.

For convenience, we will represent these functions as components of the following vectors:

$$\overline{X}^n = \{X_\pi^n(x)\}_{\substack{p=\overline{1,2,3;} \\ i=\overline{1,M}}} = \{X_{11}^n(x) \ldots X_{1M}^n(x) X_{21}^n(x) \ldots X_{2M}^n(x) X_{31}^n(x) \ldots X_{3M}^n(x)\}, \tag{1.5}$$

$$\overline{Y}^n = \{Y_\pi^n(y)\}_{\substack{p=\overline{1,2,3;} \\ i=\overline{1,M}}} = \{Y_{11}^n(y) \ldots Y_{1M}^n(y) Y_{21}^n(y) \ldots Y_{2M}^n(y) Y_{31}^n(y) \ldots Y_{3M}^n(y)\}, \tag{1.6}$$

$$\overline{Z}^n = \{Z_\pi^n(z)\}_{\substack{p=\overline{1,2,3;} \\ i=\overline{1,M}}} = \{Z_{11}^n(z) \ldots Z_{1M}^n(z) Z_{21}^n(z) \ldots Z_{2M}^n(z) Z_{31}^n(z) \ldots Z_{3M}^n(z)\}. \tag{1.7}$$

Each of the vectors $\overline{X}^n$, $\overline{Y}^n$, $\overline{Z}^n$ consists of functions of only one of the arguments x, y or z. Therefore, they are called argument vector functions, as in [4, 5]. Thus, according to (1.4), three unknown argument vector functions $\overline{X}^n$, $\overline{Y}^n$, $\overline{Z}^n$ are introduced instead of the sought vector function $\overline{V}^n$.

To determine the vector functions $\overline{X}^n$, $\overline{Y}^n$, $\overline{Z}^n$ (1.5)–(1.7), we set up a system of three one-dimensional problems. To this end, we will use a reduction procedure $P = \{P_x, P_y, P_z\}$. Each of its components is the ordinary operation of reduction to ordinary differential equations, including weighted integration over all the variables of the domain except one (projection onto different coordinate directions):

$$P_x(\cdot) = \int_0^b \int_0^c (\cdot) Y_{pk} Z_{pk} \, dydz,$$

$$P_y(\cdot) = \int_0^a \int_0^c (\cdot) X_{pk} Z_{pk} \, dxdz,$$

$$P_z(\cdot) = \int_0^a \int_0^b (\cdot) X_{pk} Y_{pk} \, dxdy, \tag{1.8}$$

where approximating functions are used as weights, as in the Galerkin method.

Applying operations (1.8) to the equations and boundary conditions of the boundary-value problem (1.2) and considering (1.4), we get a system of one-dimensional problems for the vector functions $\overline{X}^n$, $\overline{Y}^n$, $\overline{Z}^n$:

$$\int_0^b \int_0^c ((L - \tau B)\overline{F}^n - B\overline{F}^{n-1}) Y_{pk}^n Z_{pk}^n \, dydz = 0 \to (L_x^n - \tau B_x^n)\overline{X}^n - B_x^n \overline{X}^{n-1} = 0, \qquad x \in (0,a),$$

$$\int_0^b \int_0^c (R\overline{F}_M^n) Y_{pk}^n Z_{pk}^n \, dydz = 0 \to R_{\mp x}^n \overline{X}^n = 0, \qquad x = 0, \quad x = a, \tag{1.9}$$

$$\int_0^a\int_0^c ((L-\tau B)\overline{F}^n - B\overline{F}^{n-1})X^n_{pk}Z^n_{pk}\,dxdz = 0 \to (L^n_y - \tau B^n_y)\overline{Y}^n - B^n_y\overline{Y}^{n-1} = 0, \qquad y \in (0,b),$$

$$\int_0^a\int_0^c (R\overline{F}^n_M)X^n_{pk}Z^n_{pk}\,dxdz = 0 \to R^n_{\mp y}\overline{Y}^n = 0, \qquad y = 0, \quad y = b, \tag{1.10}$$

$$\int_0^a\int_0^b ((L-\tau B)\overline{F}^n - B\overline{F}^{n-1})X^n_{pk}Y^n_{pk}\,dxdy = 0 \to (L^n_z - \tau B^n_z)\overline{Z}^n - B^n_z\overline{Z}^{n-1} = 0, \qquad z \in (0,c),$$

$$\int_0^a\int_0^b (R\overline{F}^n_M)X^n_{pk}Y^n_{pk}\,dxdy = 0 \to R^n_{\mp z}\overline{Z}^n = 0, \qquad z = 0, \quad z = c, \tag{1.11}$$

where $L^n_x = \{l_{sp}\}_{s,p=1,2,3}$ is a block matrix whose blocks $l_{sp} = \{l^{sp}_{ik}\}_{i,k=\overline{1,M}}$ are matrix differential operators of the second order with respect to the variable x:

$$l^{sp}_{ik} = A^{sp}_{2ik}\frac{d^2}{dx^2} + A^{sp}_{1ik}\frac{d}{dx} + A^{sp}_{0ik}, \tag{1.12}$$

$B^n_x = \left\{ b^{ss}_{ik} \right\}_{\substack{s=1,2,3 \\ i,k=\overline{1,M}}}$ is a block-diagonal matrix.

The matrix operator of boundary conditions (the sign "–" refers to $x = 0$, and the sign "+" to $x = a$) is expressed in a similar way:

$$R^n_{\mp x} = \left\{ r^{sp}_{\mp ik} = r^{sp}_{\mp 1ik}\frac{d}{dx} + r^{sp}_{\mp 0ik} \right\}. \tag{1.13}$$

By virtue of (1.8), the coefficients in (1.12) and (1.13) depend on the functions Y^n_{pk} and Z^n_{pk}. Let us present, for illustration, the expressions of the nonzero coefficients in (1.12) for a homogeneous isotropic body (the superscript "n" is omitted):

$$A^{11}_{2ik} = 2G\frac{1-\mu}{1-2\mu}\int_0^b\int_0^c Y_{1i}Y_{1k}Z_{1i}Z_{1k}\,dydz,$$

$$A^{11}_{0ik} = -G\left(\int_0^b\int_0^c Y'_{1i}Y'_{1k}Z_{1i}Z_{1k}\,dydz + \int_0^b\int_0^c Y_{1i}Y_{1k}Z'_{1i}Z'_{1k}\,dydz)\right),$$

$$A^{12}_{1ik} = G\left(\frac{2\mu}{1-2\mu}\int_0^b\int_0^c Y'_{2i}Y_{1k}Z_{2i}Z_{1k}\,dydz - \int_0^b\int_0^c Y_{2i}Y'_{1k}Z_{2i}Z_{1k}\,dydz\right),$$

$$A^{13}_{1ik} = G\left(\frac{2\mu}{1-2\mu}\int_0^b\int_0^c Y_{3i}Y_{1k}Z'_{3i}Z_{1k}\,dydz - \int_0^b\int_0^c Y_{3i}Y_{1k}Z_{2i}Z'_{1k}\,dydz\right),$$

$$A^{21}_{1ik} = -G\left(\frac{2\mu}{1-2\mu}\int_0^b\int_0^c Y_{1i}Y'_{2k}Z_{1i}Z_{2k}\,dydz - \int_0^b\int_0^c Y'_{1i}Y_{2k}Z_{1i}Z_{2k}\,dydz\right),$$

$$A_{2ik}^{22}=G\int_0^b\int_0^c Y_{2i}Y_{2k}Z_{2i}Z_{2k}\,dydz,$$

$$A_{0ik}^{22}=-G\left(\frac{2(1-\mu)}{1-2\mu}\int_0^b\int_0^c Y'_{2i}Y'_{2k}Z_{2i}Z_{2k}\,dydz+\int_0^b\int_0^c Y_{2i}Y_{2k}Z'_{2i}Z'_{2k}\,dydz\right),$$

$$A_{0ik}^{23}=-G\left(\frac{2\mu}{1-\mu}\int_0^b\int_0^c Y_{3i}Y'_{2k}Z'_{3i}Z_{2k}\,dydz+\int_0^b\int_0^c Y'_{3i}Y_{2k}Z_{3i}Z'_{2k}\,dydz\right),$$

$$A_{1ik}^{31}=-G\left(\frac{2\mu}{1-2\mu}\int_0^b\int_0^c Y_{1i}Y_{3k}Z_{1i}Z'_{3k}\,dydz-\int_0^b\int_0^c Y_{1i}Y_{3k}Z'_{1i}Z_{3k}\,dydz\right),$$

$$A_{0ik}^{32}=-G\left(\frac{2\mu}{1-2\mu}\int_0^b\int_0^c Y'_{2i}Y_{3k}Z_{2i}Z'_{3k}\,dydz+\int_0^b\int_0^c Y_{2i}Y'_{3k}Z'_{2i}Z_{3k}\,dydz\right),$$

$$A_{2ik}^{33}=G\int_0^b\int_0^c Y_{3i}Y_{3k}Z_{3i}Z_{3k}\,dydz,$$

$$A_{0ik}^{33}=-G\left(\frac{2(1-\mu)}{1-2\mu}\int_0^b\int_0^c Y_{3i}Y_{3k}Z'_{3i}Z'_{3k}\,dydz+\int_0^b\int_0^c Y'_{3i}Y'_{3k}Z_{3i}Z_{3k}\,dydz\right). \tag{1.14}$$

The block-diagonal matrix $B_x^n=\left\{b_{ik}^{ss}\right\}_{\substack{s=1,2,3\\ i,k=\overline{1,M}}}$ has the following elements:

$$b_{ik}^{11}=\int_0^b\int_0^c \rho Y_{1i}Y_{1k}Z_{1i}Z_{1k}\,dydz,\qquad b_{ik}^{22}=\int_0^b\int_0^c \rho Y_{2i}Y_{2k}Z_{2i}Z_{2k}\,dydz,\qquad b_{ik}^{33}=\int_0^b\int_0^c \rho Y_{3i}Y_{3k}Z_{3i}Z_{3k}\,dydz.$$

The operators with subscripts y and z in (1.10) and (1.11) have the same structure, with the only difference that the differentiation in L_y^n and $R_{\mp y}$ is with respect to the variable y and the differentiation in L_z^n and $R_{\mp z}$ is with respect to the variable z, while the coefficients in the differential operators depend on the components of the vector functions $\overline{X}$ and $\overline{Z}$ in the first problem and on the components of $\overline{X}$ and $\overline{Y}$ in the second problem.

For example, we have

$$A_{2ik}^{11}=G\int_0^a\int_0^c X_{1i}X_{1k}Z_{1i}Z_{1k}\,dxdz,$$

……

$$A_{0ik}^{33}=-G\left(\frac{2(1-\mu)}{1-2\mu}\int_0^a\int_0^c X_{3i}X_{3k}Z'_{3i}Z'_{3k}\,dxdz+\int_0^a\int_0^c X'_{3i}X'_{3k}Z_{3i}Z_{3k}\,dxdz\right) \tag{1.15}$$

in problem (1.10) and

$$A_{2ik}^{11}=G\int_0^a\int_0^b X_{1i}X_{1k}Y_{1i}Y_{1k}\,dxdy,$$

……

$$A_{0ik}^{33} = -G\left(\int_0^a \int_0^b X_{3i} X_{3k} Y'_{3i} Y'_{3k}\, dxdy + \int_0^a \int_0^b X'_{3i} X'_{3k} Y_{3i} Y_{3k}\, dxdy \right) \tag{1.16}$$

in problem (1.11).

Thus, each one-dimensional problem in (1.9)–(1.11) is a system of $3\times M$ ordinary differential equations of the second order for $3\times M$ functions of one variable with appropriate boundary conditions. One-dimensional problems with respect to different variables of the domain are related by coefficients (1.14)–(1.16).

To solve the system of one-dimensional problems (1.9)–(1.11) at each step of the method of successive approximations (parameter n), the following iterative scheme (parameter $m = 1, 2, \ldots$) can be used:

$$(L_x^{n,m-1} - \tau B_x^{n,m-1})\overline{X}^{n,m} - B_x^{n,m-1}\overline{X}^{n-1,m-1} = 0, \qquad x \in (0, a),$$

$$R_{\mp x}^{n,m-1}\overline{X}^{n,m} = 0, \qquad x = 0,\ a, \tag{1.17}$$

$$(L_y^{n,m-1} - \tau B_y^{n,m-1})\overline{Y}^{n,m} - B_y^{n,m-1}\overline{Y}^{n-1,m-1} = 0, \qquad y \in (0, b),$$

$$R_{\mp y}^{n,m-1}\overline{Y}^{n,m} = 0, \qquad y = 0,\ b, \tag{1.18}$$

$$(L_z^{n,m} - \tau B_z^{n,m})\overline{Z}^{n,m} - B_z^{n,m}\overline{Z}^{n-1,m-1} = 0, \qquad z \in (0, c),$$

$$R_{\mp z}^{n,m}\overline{Z}^{n,m} = 0, \qquad z = 0,\ c. \tag{1.19}$$

The index $(m-1)$ in the operators $L_x^{n,m-1}$, $B_x^{n,m-1}$, $R_{\mp x}^{n,m-1}$ in (1.17) at the current mth step means that the functions Y_π and Z_π ($p = 1, 2, 3$, $i = \overline{1, M}$) for the calculation of the coefficients by formulas (1.14) are taken from the previous $(m-1)$th step. These indices have the same meaning in the other operators of (1.17)–(1.19).

Thus, the frequency parameter λ and associated vector function $\overline{U}$ can be determined as the limit of the functional sequence $\overline{V}^n$ ($\overline{V}^n \to \overline{U}$, $n \to \infty$) by running two nested iteration processes: an outer loop to generate the sequence $\overline{V}^n$ by the inverse-iteration method (the sequence of the boundary-value problems (1.2), parameter n) and an inner loop to solve a single problem from this sequence to determine the vector function $\overline{V}^n$ (system (1.17)–(1.19); fixed parameters m and n). Thus, we may generate the following iteration process to solve the original problem (1.1) (parameter $j = 1, 2, \ldots$):

$$(L_x^{j-1} - \tau B_x^{j-1})\overline{X}^{j} - B_x^{j-1}\overline{X}^{j-1} = 0, \qquad x \in (0, a),$$

$$R_{\mp x}^{j-1}\overline{X}^{j} = 0, \qquad x = 0,\ a, \tag{1.20}$$

$$(L_y^{j-1} - \tau B_y^{j-1})\overline{Y}^{j} - B_y^{j-1}\overline{Y}^{j-1} = 0, \qquad y \in (0, b),$$

$$R_{\mp y}^{j-1}\overline{Y}^{j} = 0, \qquad y = 0,\ b, \tag{1.21}$$

$$(L_z^{j} - \tau B_z^{j})\overline{Z}^{j} - B_z^{j}\overline{Z}^{j-1} = 0, \qquad z \in (0, c),$$

$$R_{\mp z}^{j}\overline{Z}^{j} = 0, \qquad z = 0,\ c. \tag{1.22}$$

As the initial approximation for the functions X_π^0, Y_π^0, Z_π^0 ($p = 1, 2, 3$, $i = \overline{1, M}$), we choose any functions linearly independent in i (for example, power or trigonometric). A one-dimensional boundary-value problem is solved by the orthogonal-sweep method. In some special cases, the solution can be found analytically (for example, a two-dimensional problem of plate bending for $M = 1$).

TABLE 1

Boundary conditions	Frequency No	Methods		
		AKM	[15]	[12, 16]
(i)	1	12.426	12.426	12.426
	2	18.210	18.210	18.210
	3	23.007	23.008	—
	4	25.753	25.753	—
(ii)	1	15.286	15.286	15.294
	2	24.069	24.071	24.078
	3	24.792	24.816	24.823
	4	29.377	29.376	29.377
	5	31.500	31.502	31.510
	6	35.308	35.304	35.308
	7	35.764	35.756	35.763

The iteration process of solving system (1.20)–(1.22) with a fixed number of terms M is terminated once $|1-\lambda_{n-1}/\lambda_n| \le \varepsilon$, where ε is the error of calculation.

The accuracy of the calculated natural frequency λ is improved by increasing the number of terms M in (1.4). The minimum eigenvalue $\lambda_{\min}$ is found setting $\tau = 0$, while the subsequent values of λ are found by scanning the parameter $\tau > 0$.

2. Discussion of the Numerical Results. The developed method was validated inductively by comparing solutions for specific examples found by other methods. We will compare the values of the frequency parameter $\Omega_* = \omega b^2 \sqrt{\rho c / D}$ ($D = Ec^3/12(1-\mu^2)$) [15] for a parallelepiped with square base ($b/a = 1$) and height $c/a = 0.5$. The examples chosen cover the following boundary conditions on the lateral faces $x = 0, a$, $y = 0, b$:

(i) Navier boundary conditions on all lateral faces:

$$u_2 = u_3 = 0, \quad \sigma_{11} = 0 \quad \text{at} \quad x = 0, a,$$

$$u_1 = u_3 = 0, \quad \sigma_{22} = 0 \quad \text{at} \quad y = 0, b,$$

(ii) all lateral faces are clamped:

$$u_1 = u_2 = u_3 = 0 \quad \text{at} \quad x = 0, a, \quad y = 0, b,$$

(iii) two opposite faces are clamped, and the other two are free:

$$u_1 = u_2 = u_3 = 0 \quad \text{at} \quad x = 0, a,$$

$$\sigma_{22} = \sigma_{21} = \sigma_{23} = 0 \quad \text{at} \quad y = 0, b,$$

(iv) the face $x = 0$ is clamped, the others are free:

TABLE 2

Boundary conditions	Frequency No	Methods		
		AKM	[15]	[12]
(iii)	1	10.577	10.582	10.583
	2	11.440	11.448	11.450
	3	11.768	11.769	11.770
	4	18.469	18.466	18.466
	5	20.684	20.682	20.684
	6	21.130	21.137	21.140
	7	21.643	21.641	21.642
	8	22.503	22.502	22.504
(iv)	1	2.9331	2.9331	2.9372
	2	4.3889	4.3865	4.3910
	3	5.1934	5.1925	5.1944
	4	10.516	10.516	10.548
	5	10.937	10.937	10.942
	6	11.708	11.708	11.708
	7	14.602	14.599	14.602
	8	15.026	15.024	15.024
	9	18.479	18.478	18.478
	10	20.099	20.096	20.103

$$u_1 = u_2 = u_3 = 0 \quad \text{at} \quad x = 0,$$

$$\sigma_{11} = \sigma_{12} = \sigma_{13} = 0 \quad \text{at} \quad x = a,$$

$$\sigma_{22} = \sigma_{21} = \sigma_{23} = 0 \quad \text{at} \quad y = 0, b.$$

The face planes $z = 0, c$ are free of stresses:

$$\sigma_{33} = \sigma_{13} = \sigma_{23} = 0 \quad \text{at} \quad z = 0, c.$$

The values of the parameter Ω_* for several lowest frequencies obtained using the AKM, the exact solution [16], the Ritz method with approximation by B-splines [15] and orthogonal polynomials [12] are collected in Table 1 for the boundary conditions (i) and (ii) and in Table 2 for the boundary conditions (iii) and (iv). Note that comparison is made with the exact solution [16] in case (i) and with the results [12] in case (ii).

TABLE 3

Boundary conditions	c/a	Frequency No	Methods	Ω_*	M
(i)	0.5	1	AKM	12.426	1
			[15]	12.426	7×7×9 = 441
		5	AKM	23.007	1
			[15]	23.008	7×7×9 = 441
		10	AKM	28.792	1
			[15]	28.793	7×7×9 = 441
		100	AKM	64.546	3
			[15]	64.546	11×11×9 = 1089
(ii)	0.4	1	AKM	18.081	5
			[15]	18.081	15×15×9 = 2025
		5	AKM	31.014	5
			[15]	31.014	13×13×9 = 1521
		10	AKM	44.944	5
			[15]	44.943	11×11×9 = 1089

The last two columns of Table 1 (boundary conditions (ii)) and Table 2 show that the frequencies found by the Ritz method with continuous approximation by orthogonal polynomials [12] and approximation by B-splines [15] differ by less than 0.1%.

The difference between the frequencies found by the AKM and Ritz method [12, 15] is within the same limits, which indicates that the AKM can be used to analyze the vibrations of a parallelepiped with various boundary conditions.

The comparative efficiency of the proposed method and Ritz method with B-spline approximation can be judged from the number of terms M retained to achieve the prescribed accuracy. These data are summarized in Table 3 for hinged ($c / a = 0.5$) and clamped ($c / a = 0.4$) faces (the number of terms for the other boundary conditions are not given in [15]).

As follows from Table 3, for hinged lateral faces and even highest frequencies, the AKM requires one to three terms, whereas the B-spline approximation uses two orders of magnitude more terms. The situation is the same when the faces are clamped. Thus, the AKM uses much less (by more than two orders of magnitude) basis functions because the components of the approximating expression are found by solving the problem posed.

3. Analysis of the Natural Frequencies of a Cantilever Beam. The above problem for a parallelepiped with fixed dimensions and boundary conditions was used for the purpose of comparison of different methods. A more general and complicated problem is to analyze the frequency dependence of some characteristics of an elastic body. In what follows, we will analyze the dependence of the natural frequencies of a three-dimensional cantilever beam on its cross-sectional dimensions.

Consider an isotropic beam with a rectangular cross-section occupying a Cartesian domain $\Omega \cup \partial\Omega = \{x, y, z: x \in [0, l], y \in [0, b], z \in [0, c]\}$. The beam axis is aligned with the x-axis, the face $x = 0$ is clamped, all the other faces are free. Let us analyze

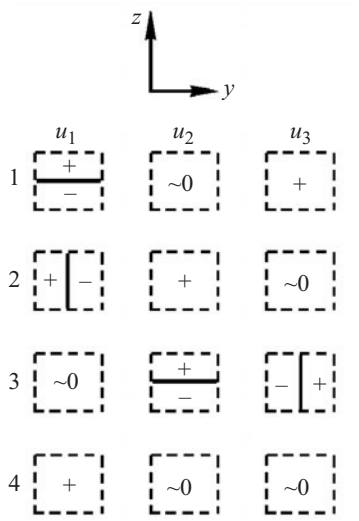

Fig. 1

the dependence of the lowest natural frequencies of the beam with fixed length l on the relative dimensions of its cross-section with constant area $S = b \times c = \text{const}$. The relative dimensions of the cross-section are characterized by the dimensionless parameter $\alpha = c / b$ varying within $\alpha \in [1.0, 0.1]$ ($\alpha = 1$ corresponds to a beam of square cross-section, while $\alpha = 0.1$ to a plate with thickness c and plan dimensions $l \times b$).

The result is spectral curves $\lambda = \lambda(\alpha)$, which show how the beam frequency varies with the parameter α for a certain vibration mode ($\lambda = \omega(\alpha) / \omega_{\min}$ (1, 0) are frequencies divided by the minimum frequency of the beam with square cross-section).

The classification of vibration modes of a spatial body should be commented. The eigenfunctions of a two-dimensional problem, as characteristics of natural modes, are usually classified according to the number of nodal lines, which is natural for scalar functions (for example, bending vibrations of a plate). In the case of the vector problem under consideration, the classification can be made according to the components of the vector eigenfunction, which are scalar functions $u_1(x, y, z)$, $u_2(x, y, z)$, and $u_3(x, y, z)$.

Each of them has its own system of nodal lines in the cross-sections of the beam. The information on the signs of shifts in these functions is used to rank the spectral properties of the beam according to the natural modes.

Depending on the number of sign reversals along the beam length in the functions $u_1(x, y, z)$, $u_2(x, y, z)$, and $u_3(x, y, z)$, there are the following sets of spectral curves: I (no sign reversal), II (one sign reversal), III (two sign reversals), etc. In each of these sets, we consider four spectral curves classified according to the pattern of nodal lines of the functions $u_1(x, y, z)$, $u_2(x, y, z)$, and $u_3(x, y, z)$ in the cross-sectional plane yz (Fig. 1):

1 — mainly bending vibrations about the y-axis; each beam section $x = x^* = \text{const}$ shifts as a single whole along the z-axis;

2 — similar vibrations about the z-axis; each beam section $x = x^* = \text{const}$ shifts as a single whole along the y-axis;

3 — shear vibrations in the plane $x = x^* = \text{const}$;

4 — piston-like vibrations along the beam.

The spectral curves of the first two sets in coordinates λ, α are given in Fig. 2 for the following initial data: $b = 10 l_0$, $c = \alpha b$, $\alpha \in [1.0, 0.1]$, $l = 2.5b|_{\alpha=1}$, $E = E_0$, $\mu = 0.3$. Here the sets of curves are denoted by Roman numerals; the curves within a set are denoted by Arabic numerals; the fourth curve of set II is omitted; l_0 is the typical linear scale.

All the curves monotonically decrease with decreasing parameter α, following the variation in the section modulus.

For example, the spectral curves for bending vibrations about the y-axis (I.1) and shear vibrations (I.3) decrease, which is consistent with the behavior of the sectional modulus of bending about the same axis $\Re_y = bc^2 / 6$ and the sectional modulus of twisting $\Re_{yz} \sim pc^3$. The frequencies of bending vibrations about the z-axis (spectral curve I.2) increase with $\Re_z = b^2 c / 6$. The piston-like frequency (curve I.4) is independent of the cross-sectional dimensions.

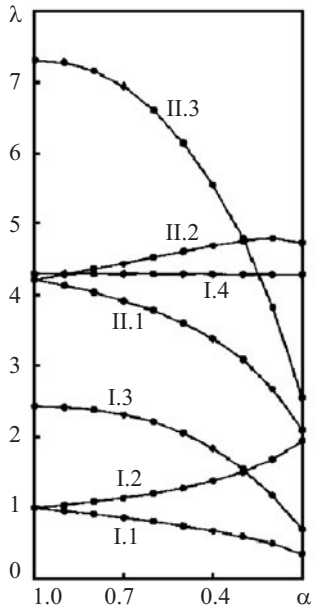

Fig. 2

TABLE 4

α	Frequency	ω^*				
		$M = 1$	$M = 2$	$M = 3$	$M = 4$	$M = 5$
1.0	I.1	1.561	1.485	1.480	1.478	1.478
0.7	I.4	6.365	6.347	6.343	6.342	6.342
0.5	II.3	9.333	9.134	9.110	9.096	9.096
0.1	II.2	7.127	7.012	7.007	7.006	7.006

Noteworthy is the presence of multiple frequencies of the beam within the examined range of variation in its cross-sectional dimensions.

They are frequencies of bending vibrations of the square beam about the *y*- and *z*-axes of each set, which is due to its geometry (I.1; I.2 and II.1; II.2 for $\alpha = 1$).

For $\alpha = 0.9$, the frequencies of the piston-like mode of the first set (I.4) and of the second mode of the second set (II.2) are multiple. For $\alpha = 0.3$, the frequencies of bending vibrations of both sets (I.2; II.2) about the *z*-axis are equal to those of shear vibrations (I.3; II.3), respectively. For $\alpha = 0.25$, the frequencies of shear vibrations of the second set (II.3) are equal to the frequencies of the piston-like mode of the first set (I.4).

In conclusion, let us demonstrate the accuracy of computation for this specific problem. Table 4 collects the dimensionless frequencies $\omega^* = \omega\sqrt{\frac{\rho}{E}}l_0 \cdot 10^2$ for different relative dimensions of the domain (α = 1.0, 0.7, 0.5, 0.1) and for various frequencies of both sets (I.1; I.4; II.3; II.2) depending on the number M of terms retained in (I.4). The solution of the static problem was used as the initial approximation for the inverse-iteration method.

As is seen from Table 4, with four to five terms of approximation, the frequencies stabilize in four decimal places in all cases. The error of the one-term approximation relative to the stable value is approximately 5%.

Conclusions. We have proposed an approach to calculate the natural frequencies and modes of a rectangular parallelepiped with various boundary conditions. The approach rationally combines the inverse iteration and advanced Kantorovich–Vlasov methods. In contrast to the conventional Ritz method, the approach does not require a priory selection of basis functions and features the following:

(i) the natural modes are described as a superposition of functions with separated variables where all the components of the approximating expression are considered unknown;

(ii) the natural frequencies of the three-dimensional parallelepiped are determined as the limit of a numerical sequence constructed using the Rayleigh quotient and the iterative solution of the system of three interrelated one-dimensional problems.

The efficiency of the method (accuracy and the number of approximating terms) has been tested by comparing with the solutions obtained by the Ritz method with different basis functions, including B-splines.

The obtained dependences of low frequencies of a cantilever beam on its cross-sectional dimensions agree with the variation of its stiffness during deformation of different types.

REFERENCES

1. P. A. Zhilin and T. P. Il'icheva, "Spectra and modes of vibrations based on the three-dimensional theory of elasticity and plate theory," *Izv. AN USSR*, *Mekh. Tverd. Tela*, No. 2, 94–103 (1980).
2. Von L. Collatz, *Eigenvalue Problems with Engineering Applications* [in German], Akad. Verlagsges., Leipzig (1963).
3. R. C. Barta, L. F. Qian, and L. M. Chen, "Natural frequencies of thick square plates made of orthotropic, trigonal, monoclinic, hexagonal and triclinic materials," *J. Sound Vibr*., **270**, No. 4–5, 1074–1086 (2004).
4. E. I. Bespalova, "Solving stationary problems for shallow shells by a generalized Kantorovich–Vlasov method," *Int.Appl. Mech*., **44**, No. 11, 1283–1293 (2008).
5. E. I. Bespalova and G. P. Urusova, "Solving the torsion problem for anisotropic prism by the advanced Kantorovich–Vlasov method," *Int. Appl. Mech*., **46**, No. 2, 149–158 (2010).
6. Ya. M. Grigorenko, O. A. Avramenko, and S. N. Yaremchenko, "Spline-approximation solution of two-dimensional problems of statics for orthotropic conical shells in a refined formulation," *Int. Appl. Mech*., **43**, No. 11, 1218–1227 (2007).
7. A. Ya. Grigorenko and T. L. Efimova, "Using spline-approximation to solve problems of axisymmetric free vibration of thick-walled orthotropic cylinders," *Int. Appl. Mech*., **44**, No. 10, 1137–1147 (2008).
8. A. Ya. Grigorenko and S. A. Maltsev, "Natural vibrations of thin conical panels of variable thickness," *Int. Appl. Mech*., **45**, No. 11, 1221–1231 (2009).
9. Ya. M. Grigorenko, N. N. Kryukov, and N. S. Yakovenko, "Using spline functions to solve boundary-value problems for laminated orthotropic trapezoidal plates of variable thickness," *Int. Appl. Mech*., **41**, No. 4, 413–420 (2005).
10. A. W. Leissa and Z. Zhang, "On the three-dimensional vibrations of cantilevered rectangular parallelepiped," *J. Acoust. Soc. Amer*., **73**, 2013–2021 (1983).
11. M. Levinson, "Free vibrations of simply supported rectangular plates: An exact elasticity solution," *J. Sound Vibr*., **98**, 289–298 (1985).
12. K. M. Liew, K. C. Hung, and K. M. Lim, "A continuum three-dimensional vibration analysis of thick rectangular plates," *Int. J. Solids Struct*., **30**, 3357–3379 (1993).
13. W. C. Lim, "Three-dimensional vibration analysis of a cantilevered parallelepiped: exact and approximate solutions," *J. Acoust. Soc. Amer*., **106**, 3375–3381 (1999).
14. O. G. McGee and A. W. Leissa, "Three-dimensional free vibrations of thick skewed cantilevered plate," *J. Sound Vibr*., **144**, 305–322 (1991).
15. H. Nagino, T. Mikami, and T. Mizusawa, "Three-dimensional free vibration analysis of isotropic rectangular plates using the B-spline Ritz method," *J. Sound Vibr*., **317**, No. 1–2, 329–353 (2008).
16. S. Srinivas, C. V. Joga Rao, and A. K. Rao, "An exact analysis for vibration of simply-supported homogeneous and laminated thick rectangular plates," *J. Sound Vibr*., **12**, 187–199 (1970).
17. D. Zhou, Y. K. Cheung, F. T. K. Au, and S. H. Lo, "Three-dimensional vibration analysis of thick rectangular plates using Chebyshev polynomial and Ritz method," *Int. J. Solids Struct*., **39**, 6339–6353 (2002).